



## Measurement of Lambda polarization from Z decays

D. Buskalic, I. De Bonis, D. Decamp, P. Ghez, C. Goy, J.P. Lees, A. Lucotte,  
M.N. Minard, P. Odier, B. Pietrzyk, et al.

► **To cite this version:**

D. Buskalic, I. De Bonis, D. Decamp, P. Ghez, C. Goy, et al.. Measurement of Lambda polarization from Z decays. Physics Letters B, Elsevier, 1996, 374, pp.319-330. <in2p3-00001377>

**HAL Id: in2p3-00001377**

**<http://hal.in2p3.fr/in2p3-00001377>**

Submitted on 8 Apr 1999

**HAL** is a multi-disciplinary open access archive for the deposit and dissemination of scientific research documents, whether they are published or not. The documents may come from teaching and research institutions in France or abroad, or from public or private research centers.

L'archive ouverte pluridisciplinaire **HAL**, est destinée au dépôt et à la diffusion de documents scientifiques de niveau recherche, publiés ou non, émanant des établissements d'enseignement et de recherche français ou étrangers, des laboratoires publics ou privés.

# Measurement of $\Lambda$ polarization from Z decays

**The ALEPH Collaboration**

## **Abstract**

The polarization of  $\Lambda$  baryons from Z decays is studied with the ALEPH apparatus. Evidence of longitudinal polarization of  $s$  quarks from Z decay is observed for the first time. The measured longitudinal  $\Lambda$  polarization is  $P_L^\Lambda = -0.32 \pm 0.07$  for  $z = p/p_{\text{beam}} > 0.3$ . This agrees with the prediction of  $-0.39 \pm 0.08$  from the standard model and the constituent quark model, where the error is due to uncertainties in the mechanism for  $\Lambda$  production. The observed  $\Lambda$  polarization is diluted with respect to the primary  $s$  quark polarization by  $\Lambda$  baryons without a primary  $s$  quark. Measurements of the  $\Lambda$  forward-backward asymmetry and of the correlation between back-to-back  $\Lambda\bar{\Lambda}$  pairs are used to check this dilution. In addition the transverse  $\Lambda$  polarization is measured. An indication of transverse polarization, more than two standard deviations away from zero, is found along the normal to the plane defined by the thrust axis and the  $\Lambda$  direction.

*To be submitted to Physics Letters B*

# The ALEPH Collaboration

D. Buskulic, I. De Bonis, D. Decamp, P. Ghez, C. Goy, J.-P. Lees, A. Lucotte, M.-N. Minard, P. Odier, B. Pietrzyk

*Laboratoire de Physique des Particules (LAPP), IN<sup>2</sup>P<sup>3</sup>-CNRS, 74019 Annecy-le-Vieux Cedex, France*

M. Chmeissani, J.M. Crespo, M. Delfino,<sup>12</sup> I. Efthymiopoulos, E. Fernandez, M. Fernandez-Bosman, Ll. Garrido,<sup>15</sup>  
A. Juste, M. Martinez, S. Orteu, A. Pacheco, C. Padilla, F. Palla, A. Pascual, J.A. Perlas, I. Riu, F. Sanchez,  
F. Teubert

*Institut de Fisica d'Altes Energies, Universitat Autònoma de Barcelona, 08193 Bellaterra (Barcelona),  
Spain<sup>7</sup>*

A. Colaleo, D. Creanza, M. de Palma, A. Farilla, G. Gelao, M. Girone, G. Iaselli, G. Maggi,<sup>3</sup> M. Maggi, N. Marinelli,  
S. Natali, S. Nuzzo, A. Ranieri, G. Raso, F. Romano, F. Ruggieri, G. Selvaggi, L. Silvestris, P. Tempesta, G. Zito

*Dipartimento di Fisica, INFN Sezione di Bari, 70126 Bari, Italy*

X. Huang, J. Lin, Q. Ouyang, T. Wang, Y. Xie, R. Xu, S. Xue, J. Zhang, L. Zhang, W. Zhao

*Institute of High-Energy Physics, Academia Sinica, Beijing, The People's Republic of China<sup>8</sup>*

R. Alemany, A.O. Bazarko, G. Bonvicini,<sup>23</sup> M. Cattaneo, P. Comas, P. Coyle, H. Drevermann, R.W. Forty,  
M. Frank, R. Hagelberg, J. Harvey, R. Jacobsen,<sup>24</sup> P. Janot, B. Jost, E. Kneringer, J. Knobloch, I. Lehraus,  
E.B. Martin, P. Mato, A. Minten, R. Miquel, Ll.M. Mir,<sup>2</sup> L. Moneta, T. Oest, P. Palazzi, J.R. Pater,<sup>27</sup> J.-  
F. Puztaszeri, F. Ranjard, P. Rensing, L. Rolandi, D. Schlatter, M. Schmelling, O. Schneider, W. Tejessy,  
I.R. Tomalin, A. Venturi, H. Wachsmuth, A. Wagner, T. Wildish, W. Witzeling, J. Wotschack

*European Laboratory for Particle Physics (CERN), 1211 Geneva 23, Switzerland*

Z. Ajaltouni, A. Barrès, C. Boyer, A. Falvard, P. Gay, C. Guicheney, P. Henrard, J. Jousset, B. Michel, S. Monteil,  
J.-C. Montret, D. Pallin, P. Perret, F. Podlyski, J. Proriot, J.-M. Rossignol

*Laboratoire de Physique Corpusculaire, Université Blaise Pascal, IN<sup>2</sup>P<sup>3</sup>-CNRS, Clermont-Ferrand,  
63177 Aubière, France*

T. Fearnley, J.B. Hansen, J.D. Hansen, J.R. Hansen, P.H. Hansen, B.S. Nilsson, A. Wäänänen

*Niels Bohr Institute, 2100 Copenhagen, Denmark<sup>9</sup>*

A. Kyriakis, C. Markou, E. Simopoulou, I. Siotis, A. Vayaki, K. Zachariadou

*Nuclear Research Center Demokritos (NRCD), Athens, Greece*

A. Blondel, G. Bonneaud, J.C. Brient, P. Bourdon, A. Rougé, M. Rumpf, R. Tanaka, A. Valassi,<sup>6</sup> M. Verderi,  
H. Videau<sup>21</sup>

*Laboratoire de Physique Nucléaire et des Hautes Energies, Ecole Polytechnique, IN<sup>2</sup>P<sup>3</sup>-CNRS, 91128  
Palaiseau Cedex, France*

D.J. Candlin, M.I. Parsons

*Department of Physics, University of Edinburgh, Edinburgh EH9 3JZ, United Kingdom<sup>10</sup>*

E. Focardi,<sup>21</sup> G. Parrini

*Dipartimento di Fisica, Università di Firenze, INFN Sezione di Firenze, 50125 Firenze, Italy*

M. Corden, C. Georgiopoulos, D.E. Jaffe

*Supercomputer Computations Research Institute, Florida State University, Tallahassee, FL 32306-  
4052, USA<sup>13,14</sup>*

A. Antonelli, G. Bencivenni, G. Bologna,<sup>4</sup> F. Bossi, P. Campana, G. Capon, D. Casper, V. Chiarella, G. Felici,  
P. Laurelli, G. Mannocchi,<sup>5</sup> F. Murtas, G.P. Murtas, L. Passalacqua, M. Pepe-Altarelli

*Laboratori Nazionali dell'INFN (LNF-INFN), 00044 Frascati, Italy*

L. Curtis, S.J. Dorris, A.W. Halley, I.G. Knowles, J.G. Lynch, V. O'Shea, C. Raine, P. Reeves, J.M. Scarr, K. Smith, A.S. Thompson, F. Thomson, S. Thorn, R.M. Turnbull

*Department of Physics and Astronomy, University of Glasgow, Glasgow G12 8QQ, United Kingdom<sup>10</sup>*

U. Becker, C. Geweniger, G. Graefe, P. Hanke, G. Hansper, V. Hepp, E.E. Kluge, A. Putzer, B. Rensch, M. Schmidt, J. Sommer, H. Stenzel, K. Tittel, S. Werner, M. Wunsch

*Institut für Hochenergiephysik, Universität Heidelberg, 69120 Heidelberg, Fed. Rep. of Germany<sup>16</sup>*

D. Abbaneo, R. Beuselinck, D.M. Binnie, W. Cameron, P.J. Dornan, A. Moutoussi, J. Nash, J.K. Sedgbeer, A.M. Stacey, M.D. Williams

*Department of Physics, Imperial College, London SW7 2BZ, United Kingdom<sup>10</sup>*

G. Dissertori, P. Girtler, D. Kuhn, G. Rudolph

*Institut für Experimentalphysik, Universität Innsbruck, 6020 Innsbruck, Austria<sup>18</sup>*

C.K. Bowdery, T.J. Brodbeck, P. Colrain, G. Crawford, A.J. Finch, F. Foster, G. Hughes, T. Sloan, E.P. Whelan, M.I. Williams

*Department of Physics, University of Lancaster, Lancaster LA1 4YB, United Kingdom<sup>10</sup>*

A. Galla, A.M. Greene, K. Kleinknecht, G. Quast, B. Renk, E. Rohne, H.-G. Sander, P. van Gemmeren C. Zeitnitz

*Institut für Physik, Universität Mainz, 55099 Mainz, Fed. Rep. of Germany<sup>16</sup>*

J.J. Aubert,<sup>21</sup> A.M. Bencheikh, C. Benchouk, A. Bonissent,<sup>21</sup> G. Bujosa, D. Calvet, J. Carr, C. Diaconu, F. Etienne, N. Konstantinidis, D. Nicod, P. Payre, D. Rousseau, M. Talby, A. Sadouki, M. Thulasidas, K. Trabelsi

*Centre de Physique des Particules, Faculté des Sciences de Luminy, IN<sup>2</sup>P<sup>3</sup>-CNRS, 13288 Marseille, France*

I. Abt, R. Assmann, C. Bauer, W. Blum, H. Dietl, F. Dydak,<sup>21</sup> G. Ganis, C. Gotzhein, K. Jakobs, H. Kroha, G. Lütjens, G. Lutz, W. Männer, H.-G. Moser, R. Richter, A. Rosado-Schlosser, S. Schael, R. Settles, H. Seywerd, R. St. Denis, W. Wiedenmann, G. Wolf

*Max-Planck-Institut für Physik, Werner-Heisenberg-Institut, 80805 München, Fed. Rep. of Germany<sup>16</sup>*

J. Boucrot, O. Callot, A. Cordier, M. Davier, L. Dufлот, J.-F. Grivaz, Ph. Heusse, M. Jacquet, D.W. Kim,<sup>19</sup> F. Le Diberder, J. Lefrançois, A.-M. Lutz, I. Nikolic, H.J. Park,<sup>19</sup> I.C. Park,<sup>19</sup> M.-H. Schune, S. Simion, J.-J. Veillet, I. Videau

*Laboratoire de l'Accélérateur Linéaire, Université de Paris-Sud, IN<sup>2</sup>P<sup>3</sup>-CNRS, 91405 Orsay Cedex, France*

P. Azzurri, G. Bagliesi, G. Batignani, S. Bettarini, C. Bozzi, G. Calderini, M. Carpinelli, M.A. Ciocci, V. Ciulli, R. Dell'Orso, R. Fantechi, I. Ferrante, L. Foà,<sup>1</sup> F. Forti, A. Giassi, M.A. Giorgi, A. Gregorio, F. Ligabue, A. Lusiani, P.S. Marrocchesi, A. Messineo, G. Rizzo, G. Sanguinetti, A. Sciabà, P. Spagnolo, J. Steinberger, R. Tenchini, G. Tonelli,<sup>26</sup> C. Vannini, P.G. Verdini, J. Walsh

*Dipartimento di Fisica dell'Università, INFN Sezione di Pisa, e Scuola Normale Superiore, 56010 Pisa, Italy*

A.P. Betteridge, G.A. Blair, L.M. Bryant, F. Cerutti, J.T. Chambers, Y. Gao, M.G. Green, D.L. Johnson, T. Medcalf, P. Perrodo, J.A. Strong, J.H. von Wimmersperg-Toeller

*Department of Physics, Royal Holloway & Bedford New College, University of London, Surrey TW20 OEX, United Kingdom<sup>10</sup>*

D.R. Botterill, R.W. Clift, T.R. Edgecock, S. Haywood, P. Maley, P.R. Norton, J.C. Thompson, A.E. Wright  
*Particle Physics Dept., Rutherford Appleton Laboratory, Chilton, Didcot, Oxon OX11 0QX, United Kingdom<sup>10</sup>*

B. Bloch-Devaux, P. Colas, S. Emery, W. Kozanecki, E. Lançon, M.C. Lemaire, E. Locci, B. Marx, P. Perez, J. Rander, J.-F. Renardy, A. Roussarie, J.-P. Schuller, J. Schwindling, A. Trabelsi, B. Vallage

*CEA, DAPNIA/Service de Physique des Particules, CE-Saclay, 91191 Gif-sur-Yvette Cedex, France<sup>17</sup>*

R.P. Johnson, H.Y. Kim, A.M. Litke, M.A. McNeil, G. Taylor

*Institute for Particle Physics, University of California at Santa Cruz, Santa Cruz, CA 95064, USA<sup>22</sup>*

A. Beddall, C.N. Booth, R. Boswell, C.A.J. Brew, S. Cartwright, F. Combley, A. Koksai, M. Letho, W.M. Newton, C. Rankin, J. Reeve, L.F. Thompson

*Department of Physics, University of Sheffield, Sheffield S3 7RH, United Kingdom<sup>10</sup>*

A. Böhrer, S. Brandt, V. Büscher, G. Cowan, C. Grupen, G. Lutters, J. Minguet-Rodriguez, F. Rivera,<sup>25</sup> P. Saraiva, L. Smolik, F. Stephan,

*Fachbereich Physik, Universität Siegen, 57068 Siegen, Fed. Rep. of Germany<sup>16</sup>*

M. Aleppo,<sup>20</sup> M. Apollonio, L. Bosisio, R. Della Marina, G. Giannini, B. Gobbo, G. Musolino, F. Ragusa<sup>20</sup>

*Dipartimento di Fisica, Università di Trieste e INFN Sezione di Trieste, 34127 Trieste, Italy*

J. Rothberg, S. Wasserbaech

*Experimental Elementary Particle Physics, University of Washington, WA 98195 Seattle, U.S.A.*

S.R. Armstrong, L. Bellantoni,<sup>30</sup> P. Elmer, Z. Feng, D.P.S. Ferguson, Y.S. Gao, S. González, J. Grahl, T.C. Greening, J.L. Harton,<sup>28</sup> O.J. Hayes, H. Hu, P.A. McNamara III, J.M. Nachtman, W. Orejudos, Y.B. Pan, Y. Saadi, M. Schmitt, I.J. Scott, V. Sharma,<sup>29</sup> J.D. Turk, A.M. Walsh, Sau Lan Wu, X. Wu, J.M. Yamartino, M. Zheng, G. Zobernig

*Department of Physics, University of Wisconsin, Madison, WI 53706, USA<sup>11</sup>*

---

<sup>1</sup>Now at CERN, 1211 Geneva 23, Switzerland.

<sup>2</sup>Supported by Dirección General de Investigación Científica y Técnica, Spain.

<sup>3</sup>Now at Dipartimento di Fisica, Università di Lecce, 73100 Lecce, Italy.

<sup>4</sup>Also Istituto di Fisica Generale, Università di Torino, Torino, Italy.

<sup>5</sup>Also Istituto di Cosmo-Geofisica del C.N.R., Torino, Italy.

<sup>6</sup>Supported by the Commission of the European Communities, contract ERBCHBICT941234.

<sup>7</sup>Supported by CICYT, Spain.

<sup>8</sup>Supported by the National Science Foundation of China.

<sup>9</sup>Supported by the Danish Natural Science Research Council.

<sup>10</sup>Supported by the UK Particle Physics and Astronomy Research Council.

<sup>11</sup>Supported by the US Department of Energy, grant DE-FG0295-ER40896.

<sup>12</sup>Also at Supercomputations Research Institute, Florida State University, Tallahassee, U.S.A.

<sup>13</sup>Supported by the US Department of Energy, contract DE-FG05-92ER40742.

<sup>14</sup>Supported by the US Department of Energy, contract DE-FC05-85ER250000.

<sup>15</sup>Permanent address: Universitat de Barcelona, 08208 Barcelona, Spain.

<sup>16</sup>Supported by the Bundesministerium für Forschung und Technologie, Fed. Rep. of Germany.

<sup>17</sup>Supported by the Direction des Sciences de la Matière, C.E.A.

<sup>18</sup>Supported by Fonds zur Förderung der wissenschaftlichen Forschung, Austria.

<sup>19</sup>Permanent address: Kangnung National University, Kangnung, Korea.

<sup>20</sup>Now at Dipartimento di Fisica, Università di Milano, Milano, Italy.

<sup>21</sup>Also at CERN, 1211 Geneva 23, Switzerland.

<sup>22</sup>Supported by the US Department of Energy, grant DE-FG03-92ER40689.

<sup>23</sup>Now at Wayne State University, Detroit, MI 48202, USA.

<sup>24</sup>Now at Lawrence Berkeley Laboratory, Berkeley, CA 94720, USA.

<sup>25</sup>Partially supported by Colciencias, Colombia.

<sup>26</sup>Also at Istituto di Matematica e Fisica, Università di Sassari, Sassari, Italy.

<sup>27</sup>Now at Schuster Laboratory, University of Manchester, Manchester M13 9PL, UK.

<sup>28</sup>Now at Colorado State University, Fort Collins, CO 80523, USA.

<sup>29</sup>Now at University of California at San Diego, La Jolla, CA 92093, USA.

<sup>30</sup>Now at Fermi National Accelerator Laboratory, Batavia, IL 60510, USA.

# 1 Introduction

In this letter a measurement of the longitudinal and transverse polarization of  $\Lambda$  baryons in  $Z$  decays is presented. The  $\Lambda$  polarization is measured from the decay  $\Lambda \rightarrow p\pi^-$  (charge conjugation is implied throughout the text) using data collected with the ALEPH apparatus from 1991 to 1994.

In the standard model down-type quarks from  $Z$  decay are strongly lefthanded. In the simple quark picture of  $\Lambda$  baryons, the  $\Lambda$  spin is that of its constituent  $s$  quark and primary  $s$  quarks will transmit all of their polarization to the directly produced  $\Lambda$ 's. On the other hand  $\Lambda$ 's produced from primary  $u$  or  $d$  quarks as well as  $\Lambda$ 's coming from secondary fragmentation processes are not expected to be longitudinally polarized.

In order to estimate the fraction of  $\Lambda$ 's containing a primary quark or a quark from the weak decay of a heavy quark, the  $\Lambda$  forward-backward asymmetry and the correlation between high-energy back-to-back  $\Lambda\bar{\Lambda}$  pairs are measured. The fraction of  $\Lambda$ 's with a primary  $s$  quark is taken from JETSET [1], which also provides the probability that a  $\Lambda$  has resulted from the decay of a heavier baryon. The  $\Lambda$  polarization from decays of hyperons with a primary  $s$  quark has been estimated [2] using the constituent quark model. Within the uncertainties of the  $\Lambda$  production mechanism, estimated from comparisons with data, the standard model and the constituent quark model provide a prediction of the longitudinal  $\Lambda$  polarization that can be compared with the measurement.

It is well known that the constituent quark picture disagrees with the sum of quark spins in the nucleons measured in polarized deep inelastic scattering [3]. However, the deviations from the quark model prediction are localized at small momentum fraction  $x$ . At high  $x$  the deep inelastic data agree well with the model, and this is also the case for the differences between hyperon magnetic moments [4]. It is therefore possible that the polarized fragmentation functions will agree with the model for baryons at high  $z$ , where  $z$  is the fraction of the primary quark momentum carried by the baryon.

Transverse polarization perpendicular to the production plane has been observed in inclusive  $\Lambda$  production from hadron collisions since the 1960's [5]. In  $e^+e^-$  collisions the mechanism for  $\Lambda$  production is different. It is not excluded, however, that transverse polarization could arise from final state interactions [6], although no quantitative prediction is available so far. A quantitative prediction is available for transverse spin-spin correlations at the quark level [7, 8, 9]. In order to observe the effect in hadronic events, the use of back-to-back  $\Lambda\bar{\Lambda}$  pairs has been suggested [9] and is investigated in this paper.

## 2 The ALEPH detector

The ALEPH detector has been described in detail elsewhere [10]. For this study it is mainly the tracking capability of the detector that is relevant. Charged tracks are measured over the polar angle range  $|\cos\theta| < 0.97$  by an inner cylindrical drift chamber and a cylindrical time projection chamber (TPC) immersed in an axial magnetic field of 1.5 T. The properties of the TPC are essential for the measurement of high energy  $\Lambda$  decays: radial coverage out to 1.8 m and up to 21 three-dimensional coordinates per track with a spatial precision of  $173\ \mu\text{m}$  transverse to the beam axis and  $740\ \mu\text{m}$  along the beam axis [11]. Central tracks are in addition measured by a vertex detector made of two barrels of silicon microstrip detectors with double-sided readout, situated at 6.5 and 11.3 cm from the beam axis and extending to  $|\cos\theta| = 0.84$  and 0.69. For dimuon events

the momentum resolution is  $\delta p/p = 0.0006 \cdot p \text{ (GeV}/c)^{-1} \oplus 0.005$  when all tracking detectors are used.

The TPC provides up to 338 measurements of the specific ionization,  $dE/dx$ , for each charged track. For charged tracks with momenta above 3 GeV/ $c$  and with the maximum number of samples, the truncated mean ionization of pions and protons are separated by three standard deviations [11].

### 3 Selection and analysis of $\Lambda \rightarrow p\pi^-$ decays

A sample of three million hadronic events recorded over the years 1991-1994 is selected as described in [12]. In these events all oppositely charged pairs of tracks with momenta larger than 200 MeV/ $c$  and with at least five TPC coordinates are fitted to the hypothesis that they originate from the decay of a  $\Lambda$  whose line of flight intersects the beam axis [13]. The fitted parameters are the  $\Lambda$  momentum, the decay vertex and decay angles and the  $z$  coordinate of the primary vertex. Since each track is described by five helix parameters, the fit has three degrees of freedom.

A series of cuts is then applied to the sample of  $\Lambda$  candidates in order to suppress combinatorial and  $K^0$  background. The  $\chi^2$  of the fit must be less than 24. The mass pull,  $|M_{\text{meas}} - M_{\Lambda}|/\sigma_M$ , where  $\sigma_M$  is the resolution on the measured mass, must be less than four. The proper decay time must be between 0.1 and 5 times the mean lifetime. Pairs of tracks from the primary vertex are suppressed by the requirement that the two tracks be separated by at least 0.2 cm at their closest approach to the beam axis in the perpendicular plane. The cosine of the decay angle must be less than 0.95. If more than one  $V^0$  hypothesis is available for the same charged tracks, a choice is made between them. In some cases two  $\Lambda$  fits are available sharing both tracks, but with different decay vertex positions. The vertex closest to the primary vertex is chosen if there are hits between the two vertices, and the far vertex is chosen if there are no hits and some detector layers are crossed in between the two vertices. If the hit pattern offers no guidance, the fit with the best  $\chi^2$  is chosen.

The specific ionization is used to further suppress the  $K^0$ 's. The  $dE/dx$  of the proton track must not exceed the expected  $dE/dx$  by more than two  $\sigma$ . The ionization measured on the pion track must be within three  $\sigma$  of the expectation. The  $dE/dx$  requirement is only made if at least 50 ionization samples are measured on the track with the TPC. If both a  $K^0$  fit and a  $\Lambda$  fit are available for the two tracks, the hypothesis most consistent with the  $dE/dx$  measurement is chosen. If this measurement cannot be used, the hypothesis with the smallest mass pull is chosen.

The same selection procedure is applied to a sample of three million Monte Carlo events based on the event generators DYMU [14] and JETSET 7.3. The JETSET parameters were tuned [15] to reproduce the ALEPH data as closely as possible. The Monte Carlo is used to estimate the background in the selected sample of  $\Lambda$  candidates and to correct for the selection efficiency. The background contamination, dominated by  $K^0$ 's, varies from 7% to 20% when the momentum fraction,  $z = p/p_{\text{beam}}$ , goes from 0.15 to 0.5. The  $K^0$  contribution in each momentum bin is scaled by the ratio of the observed  $K^0$  spectrum [12] to the generated one. Similarly, the simulated momentum distribution of  $\Lambda$ 's is weighted by an energy dependent factor in order to reproduce the measured cross section [12]. The  $\Lambda \rightarrow p\pi^-$  selection efficiency is 36% at  $z \approx 0.15$  and 13% at  $z \approx 0.5$ . The invariant mass distribution and the proton  $dE/dx$  distribution of the simulated  $\Lambda$  candidates are compared with the data at large momenta in Figure 1.

## 4 Longitudinal polarization measurement

In the parity violating decay,  $\Lambda \rightarrow p\pi^-$ , S and P wave final states interfere. As a consequence, the distribution of  $c^* = \cos \theta^*$ , where  $\theta^*$  is the angle between the  $\Lambda$  flight direction and the proton in the  $\Lambda$  rest frame, becomes

$$r(c^*) = 1 + \alpha P_L^\Lambda c^* , \quad (1)$$

where  $\alpha$  is  $0.642 \pm 0.013$  for  $\Lambda$  [4] and  $-0.642$  for  $\bar{\Lambda}$  by CP invariance, and  $P_L^\Lambda$  is the  $\Lambda$  longitudinal polarization. Since the  $\bar{s}$  quark helicity is expected to be opposite that of the  $s$  quark, we expect the same slope of the  $c^*$  distribution for  $\Lambda$  and  $\bar{\Lambda}$ . Hence  $r(c^*)$  is fitted with  $P_L^\Lambda$  as the only parameter to the distribution  $\Lambda(c^*) + \bar{\Lambda}(c^*)$ , where  $\Lambda(c^*)$  is the measured  $\Lambda$  angular distribution, corrected for background and efficiency and normalized to unit integral. The assumption of equal  $\Lambda(c^*)$  and  $\bar{\Lambda}(c^*)$  distributions is checked by fitting  $r(c^*)$  to the distribution  $\Lambda(c^*) + \bar{\Lambda}(-c^*)$  which gives the sum of the  $\Lambda$  and  $\bar{\Lambda}$  polarizations to be  $0.028 \pm 0.042$  for  $z > 0.3$  with a  $\chi^2$  per degree of freedom of 18/18. This is compatible with the expected value of zero.

The fit is good in each momentum interval. The result is shown in Figure 2a for  $z > 0.3$  where the sensitivity to polarization is expected to be large. At such large momenta the corrections applied to the data are also large, as shown in Figure 2b. In Figure 3 and Table 1 the polarization is shown as a function of momentum. Small corrections, less than 2% of the fitted polarization, are made for the precession of the  $\Lambda$  spin in the magnetic field and for the resolution of the  $c^*$  measurement. At high momentum the  $\Lambda$  longitudinal polarization is measured to be

$$P_L^\Lambda = -0.320 \pm 0.040 \pm 0.056 \quad \text{for } z > 0.3 ,$$

where the first error is statistical and the second systematic. The  $\chi^2$  per degree of freedom is 9/18 using statistical errors.

## 5 Systematic errors on the longitudinal polarization

The background contribution is taken from the Monte Carlo simulation. However, the dominant  $K^0$  component is rescaled in each momentum bin so that it agrees with the measured  $K^0$  momentum distribution. From studies of sidebands in the  $\Lambda$  mass distribution and in the proton ionization distribution, presented in Figure 1 for large momentum  $\Lambda$ 's, an uncertainty less than 10% is found in the background level for each momentum bin. Figure 1b shows that although the simulated ionization peak is slightly shifted with respect to data, the background dominated tail agrees well with data. The variation of the background fraction with decay angle is shown in Figure 2b for high momentum  $\Lambda$ 's where the background is largest. A 10% shift in this curve results in a variation in the measured longitudinal polarization as shown in column 2 of Table 2.

The decay angle dependence of the acceptance, also shown in Figure 2b, features a dip around  $\cos \theta^* = 0.2$  from kinematically ambiguous  $\Lambda/K^0$  candidates for which the  $K^0$  hypothesis is chosen. If the choice between ambiguous hypotheses is omitted, the dip disappears and the background in the sample doubles. This results in small shifts in the longitudinal polarization which are taken as the systematic errors shown in column 3 of Table 2.

The most serious potential error source is a smooth linear rise of the acceptance with  $\cos \theta^*$  for high energy  $\Lambda$ 's. This is visible in Figure 2b if the dip is ignored. An imperfect simulation of



the slope of the acceptance would directly feed into the result without increasing the  $\chi^2$  of the fit. The slope increases with the energy of the  $\Lambda$ , favouring decay pions with relatively low energy. For low energy  $\Lambda$ 's, the trend is reversed and low momentum pions are suppressed by the acceptance. The  $K^0$  acceptance has a similar dependence on the decay angle, though mirror symmetric about  $90^\circ$ . Here the corrected distribution is expected to be flat. For  $K^0$ 's with  $z > 0.2$  the slope of the corrected distribution is found to be  $+0.013 \pm 0.021$  in the interval  $0 < c^* < 1$ , while it is 0.09 before acceptance correction. Similarly, the corrected  $c^*$  distribution for converted photons in the same momentum interval is found to have a slope of  $-0.026 \pm 0.099$ , while the slope of the acceptance is 0.40. For each distribution the hypothesis of a flat shape is perfectly consistent with the data after corrections. The slope of the  $V^0$  acceptance is therefore found to be correctly simulated within a relative uncertainty of  $\pm 17\%$ , obtained by combining the two measurements of the relative difference between the simulated and true slope. The corresponding systematic uncertainties on the  $\Lambda$  polarization are listed in column 4 of Table 2. The individual experimental uncertainties are added together in quadrature in Figure 3 and in Table 1.

## 6 Predicting the $\Lambda$ longitudinal polarization

The longitudinal polarization of quarks from  $Z$  decay is well understood theoretically. It depends on the quark flavour,  $\sin^2 \theta_W$ , the polar angle and the collision energy [2]. The beam-energy and polar angle dependences are very small. Using a value of 0.2322 for  $\sin^2 \theta_W$  and  $90^\circ$  for the polar angle, an average polarization of  $-0.935$  is predicted for *down*-type quarks at the  $Z$  peak. A one-loop QCD calculation [16] shows that gluon radiation reduces the polarization of light quarks by about 3%. Thus we expect  $P_L^s = -0.91$  with an uncertainty of about 1%.

In the quark model, the polarization of a  $\Lambda$  is that of its constituent  $s$  quark. The measured sample comprises both  $\Lambda$ 's containing primary  $s$  quarks from  $Z$  decay and  $\Lambda$ 's containing  $s$  quarks produced in the fragmentation process. The latter type is expected to have no longitudinal polarization due to parity conservation in strong interactions. The fraction  $f$  of the measured  $\Lambda$  sample containing a primary quark (or a quark from a weak decay of a primary quark) is extracted directly from data using the two methods described in the following subsections. For reasons of statistics,  $f$  is measured as an average over the interval  $z > 0.15$ . The primary  $s$  quark contribution to  $f$  and the contribution to the polarization from secondary  $\Lambda$ 's are then discussed. A correction factor is determined for the JETSET or HERWIG prediction of the fraction  $f_s$  of  $\Lambda$ 's with a primary  $s$  quark. The expected polarization for these  $\Lambda$ 's is multiplied by  $f_s$  and the small contribution from weak decays is added. In this way a prediction of the longitudinal polarization is obtained together with an estimate of the uncertainty due to the  $\Lambda$  production mechanism.

### 6.1 Back-to-back correlations

The ‘‘hypercharge correlation’’ of back-to-back  $\Lambda$  pairs is defined as

$$f = \sqrt{\frac{\Lambda\bar{\Lambda} - \Lambda\Lambda - \bar{\Lambda}\bar{\Lambda}}{\Lambda\bar{\Lambda} + \Lambda\Lambda + \bar{\Lambda}\bar{\Lambda}}},$$

where  $\Lambda\Lambda$  denotes the number of events with a  $\Lambda$  in each hemisphere. This quantity directly measures the fraction of  $\Lambda$ 's with a primary quark, assuming that the probability for production of a  $\Lambda$  not containing a primary quark is the same in the quark and anti-quark hemispheres. In the data, 254 high energy pairs with  $z > 0.15$  are found with the two  $\Lambda$ 's in opposite hemispheres.

After correcting for the estimated background of  $55 \pm 8$  events, the hypercharge correlation is found to be  $f = 0.48 \pm 0.09$ . JETSET predicts a value of 0.51 and HERWIG [17] of 0.32, when the energy dependence of the acceptance over the interval  $z > 0.15$  is taken into account. Thus, the data agree with JETSET, while they favour a higher fraction of “leading”  $\Lambda$ 's than predicted by HERWIG.

## 6.2 Forward-Backward asymmetry

Let  $c = \cos \theta$  be the cosine of the  $\Lambda$  polar angle and  $\Lambda(c)$  the uncorrected rate of  $\Lambda$  candidates as a function of  $c$ . A part of the forward-backward asymmetry present at the quark level,  $A_{\text{FB}}^{\Lambda}$ , is transferred to the  $\Lambda$ 's. The asymmetry is obtained from a one-parameter fit of the function

$$r(c) = \frac{8}{3} A_{\text{FB}}^{\Lambda} \frac{c}{1 + c^2}$$

to the distribution

$$\begin{aligned} \hat{r}(c) &= \frac{\Lambda(c) - \bar{\Lambda}(c)}{\Lambda(c) + \bar{\Lambda}(c)} (1 + r_b(c)) \\ r_b(c) &= \frac{2B(c)}{\Lambda(c) + \bar{\Lambda}(c) - 2B(c)} \end{aligned}$$

where  $B(c)$  is the background contribution which has no asymmetry according to the Monte Carlo. The fit range is  $-0.9 < c < 0.9$ . The detection efficiency is expected to be equal for  $\Lambda$  and  $\bar{\Lambda}$  and to cancel out, as confirmed by a comparison between detector level simulation and hadron level simulation. Another check is performed by repeating the procedure with high energy  $K^0$ 's. Identified  $K^0 \rightarrow \pi^+\pi^-$  decays are labeled as particles if the  $\pi^+$  carries more energy than the  $\pi^-$ , and as antiparticles in the opposite case. For  $z > 0.15$  a  $K^0$  asymmetry of  $0.0008 \pm 0.0025$  is extracted from data. If the average value of  $r(c)$  is allowed to float in the fit, an excess of  $\Lambda$  over  $\bar{\Lambda}$  of  $1.0\% \pm 0.5\%$  is found. This, however, does not change the fitted values of  $A_{\text{FB}}^{\Lambda}$ . The  $\chi^2$  of the fits is 12 for 7 degrees of freedom for  $z > 0.15$  using statistical errors only. From these studies, the systematic error on  $A_{\text{FB}}^{\Lambda}$  includes a 10% variation of the background level and an additional error of 0.003 from modelling the detection efficiency.

A positive asymmetry, increasing with energy, is found in the data measured at the Z peak as shown in Figure 4 and in Table 3. There is reasonable agreement with a calculation using JETSET for the fraction of the  $\Lambda$ 's with a given primary quark constituent and a standard model fit to LEP data for the quark asymmetries,  $A_{\text{FB}}^{\text{down}} = 0.0957$  and  $A_{\text{FB}}^{\text{up}} = 0.0639$  [18]. An asymmetry of 0.0384 is predicted for  $z > 0.15$  (again taking into account the energy dependence of the  $\Lambda$  acceptance), while the measured value for  $z > 0.15$  is

$$A_{\text{FB}}^{\Lambda} = 0.0450 \pm 0.0053 .$$

For  $z > 0.3$ , a value of  $0.085 \pm 0.012$  is found. This agrees well with the value  $0.085 \pm 0.039$  recently reported by DELPHI [19] for  $0.25 < z < 0.5$ . The HERWIG generator predicts a much smaller asymmetry, which is also shown in Figure 4. The ratio between the measured and predicted asymmetries is interpreted as the ratio between the true and predicted fraction of  $\Lambda$ 's containing a primary quark.

### 6.3 Sources of polarized $\Lambda$ 's

Primary quarks in  $\Lambda$ 's are predicted by JETSET to be mostly  $s$  quarks (about 70% for  $z > 0.3$  and 50% for  $z > 0.15$ ). To estimate the uncertainty on this prediction, the ALEPH measurements of the ratio between  $\Lambda$  and proton multiplicities at  $z > 0.15$  are studied. The measured ratio is  $0.45 \pm 0.04$  [12, 20], which agrees within 10% with the JETSET prediction of 0.42. Similarly, the value of the strange diquark suppression used in the JETSET simulation is determined with a relative error of 14% from a global fit [15] of JETSET parameters to ALEPH and PETRA data. It is therefore assumed that the primary  $s$  quark contribution to the  $\Lambda$ 's containing a primary quark is correctly given by JETSET with a 14% uncertainty.

The polarization of  $\Lambda$ 's from decays of hyperons with a primary  $s$  quark constituent has been estimated [2] according to the quark model. The contribution of such secondary  $\Lambda$ 's to the measured sample is estimated with JETSET. Direct measurements of  $\Sigma$  and  $\Xi$  hyperons yield total multiplicities consistent with JETSET, except perhaps in the case of  $\Sigma^*$ , for which OPAL and DELPHI measure about half the predicted multiplicity [21, 22] whereas ALEPH finds better agreement with JETSET [23]. Therefore half of the contribution to the polarization from  $\Sigma^*$  is included in the uncertainty of the prediction. Hyperon states with orbital angular momentum are ignored.

Polarization can also be transferred to  $\Lambda$ 's from weak decays of heavy baryons. The  $\Lambda_b$  polarization has been measured to be  $-0.23_{-0.21}^{+0.25}$  [24]. The  $\Lambda_c$  polarization is expected to be smaller than the  $\Lambda_b$  polarization [25]. The large negative asymmetry parameter measured in some  $\Lambda_c$  decays [26, 27] suggests that some of the longitudinal polarization carried by heavy flavour baryons is transferred to the  $\Lambda$ 's. Even unpolarized baryons decaying weakly into  $\Lambda$ 's contribute to the  $\Lambda$  polarization because the 'trigger bias' of the high-energy  $\Lambda$  selection favours forward decays and results in a negative longitudinal polarization. The longitudinal polarization of  $\Lambda$ 's from  $\Xi$  decays is calculated to be  $-0.06$  on average, while the  $\Lambda$  polarization from heavy flavor baryon decays is assumed to be in the range  $-0.25 \pm 0.25$ . This also covers the uncertainty in the heavy quark tagging purity.

### 6.4 Longitudinal $\Lambda$ polarization prediction

The average ratio between measured and predicted values of the forward-backward asymmetry and back-to-back correlation is interpreted as a correction to the predicted contribution to the  $\Lambda$ 's from primary quarks. The average ratio between the measurements and the JETSET predictions is found to be  $1.07 \pm 0.11$  for  $z > 0.15$  (assumed to be the same at all energies). Including the estimated 14% uncertainty in the primary flavour mixture, the correction factor becomes  $1.07 \pm 0.17$ . The corresponding correction to HERWIG is  $2.17 \pm 0.27$ . All sources of  $\Lambda$ 's with a primary  $s$  quark are corrected by this factor.

The expected share of the  $\Lambda$  production from each source is multiplied by the expected  $\Lambda$  polarization shown in Table 4, and the contributions are added. An extra dilution factor ranging from 0.95 at  $z = 0.15$  to 0.99 at  $z = 0.4$  is applied to take the angle between the quark and  $\Lambda$  directions into account. The predicted polarization using both JETSET and HERWIG is shown in Figure 3 together with the estimated uncertainty. The JETSET prediction is identical to the earlier calculation [2], except for the correction factor and the contribution from weak decays. For  $z > 0.3$ , the predicted polarization is  $-0.39 \pm 0.08$  using JETSET which agrees well with the measurement. The corrected HERWIG prediction also agrees with data.

## 7 Transverse polarization measurement

The  $\Lambda$  transverse polarization is investigated along the axis  $\hat{a}$  defined by  $\hat{p}_{\text{thrust}} \times \hat{p}_{\Lambda}$ , where  $\hat{p}_{\text{thrust}}$  is the thrust axis direction in the  $\Lambda$  hemisphere and  $\hat{p}_{\Lambda}$  is the  $\Lambda$  direction. These are the two measured directions relevant for inclusive  $q \rightarrow \Lambda + X$  fragmentation. Transverse polarization could only arise from fragmentation effects, since transverse polarization of primary quarks is suppressed by a factor  $m_q/\sqrt{s}$  from helicity conservation in vector and axial vector couplings. However, final state interactions do not necessarily conserve helicity, and final state transverse polarization of hadrons is not forbidden by P and C symmetries [6].

As in the longitudinal case, the transverse polarization can be extracted from a fit of the function (1) to the distribution of  $\cos \phi_p$ , where  $\phi_p$  is the angle in the  $\Lambda$  rest frame between the proton and  $\hat{a}$ . In this case, however, the efficiency and the background is expected to be mirror symmetric around  $\cos \phi_p = 0$ . This is confirmed with an accuracy of 0.2% by the Monte Carlo simulation presented in Figure 5b. Assuming this symmetry *a priori*, it is possible to make an estimate of the transverse polarization which is almost independent of apparatus simulation. The asymmetry

$$A_T = \frac{N_{\Lambda}(\cos \phi_p) - N_{\Lambda}(-\cos \phi_p)}{N_{\Lambda}(\cos \phi_p) + N_{\Lambda}(-\cos \phi_p)},$$

where  $N_{\Lambda}$  is the measured  $\Lambda$  rate corrected for the symmetrized efficiency and background, is fitted by the function  $\alpha P_T^{\Lambda} |\cos \phi_p|$ . The result is shown in Figure 5a for  $p_T > 0.3$  GeV/ $c$ , where  $p_T$  is the transverse momentum measured relative to the thrust axis.

No significant difference between the measured  $\Lambda$  and  $\bar{\Lambda}$  polarization is found in the data. Neither is any  $p_T$  dependence observed, as shown in Table 1, nor any energy dependence. The average result for the transverse polarization of  $\Lambda$  and  $\bar{\Lambda}$  is

$$\begin{aligned} P_T^{\Lambda} &= 0.016 \pm 0.007 \quad \text{for } p_T > 0.3 \text{ GeV}/c \\ P_T^{\bar{\Lambda}} &= 0.019 \pm 0.007 \quad \text{for } p_T > 0.6 \text{ GeV}/c, \end{aligned}$$

with a  $\chi^2$  per degree of freedom of 5/9 and 3/9, respectively. The errors are statistical only. According to Figure 5b, the efficiency has a minimum at  $\cos \phi_p = 0$ . This feature is even more pronounced for  $K^0$  decays and electrons from  $\gamma$  conversions, and the simulation of the acceptance is checked by repeating the measurement for  $K^0$  candidates and converted  $\gamma$  candidates:

$$\begin{aligned} P_T^{K^0} &= -0.002 \pm 0.003 \quad \text{for } p_T > 0.3 \text{ GeV}/c \\ P_T^{\gamma} &= 0.002 \pm 0.007 \quad \text{for } p_T > 0.3 \text{ GeV}/c, \end{aligned}$$

with a  $\chi^2$  per degree of freedom of 7/9 and 8/9, respectively.

In conclusion, an indication for transverse polarization of inclusively produced  $\Lambda$ 's from Z decay is observed above the two  $\sigma$  level. It should be noted that a 100% polarization along  $\hat{p}_{\text{quark}} \times \hat{p}_{\Lambda}$  would result in a measured polarization of 85% for  $p_T > 0.3$  GeV/ $c$  due to the experimental resolution of the thrust axis direction.

In order to study transverse polarization related to the primary quarks, which is theoretically forbidden, an energy cut is applied to the  $\Lambda$  sample. The result for the polarization along the  $\hat{a}$  axis is  $P_T^{\Lambda} = 0.018 \pm 0.021$  for  $p_T > 0.3$  GeV/ $c$  and  $z > 0.15$ . If the thrust axis is replaced by the  $z$ -axis of the laboratory, thus measuring the  $\Lambda$  polarization along the normal to the scattering plane,

no significant polarization is observed:  $P_{\text{out}}^{\Lambda} = -0.011 \pm 0.016$  for  $z > 0.15$ . The net transverse polarization *in* the scattering plane, along  $\hat{p}_{\Lambda} \times (\hat{z} \times \hat{p}_{\Lambda})$ , is found to be  $P_{\text{in}}^{\Lambda} = -0.015 \pm 0.015$  for  $z > 0.15$ . A small transverse polarization of order  $-1\%$  is actually expected along those axis as a result of the Larmor precession of the longitudinal spin. In conclusion, no indication is seen for transverse polarization at the primary quark level.

Although the quarks from the decay of an intermediate boson have no net transverse polarization, the standard model predicts a correlation between the spins of the quark and the antiquark [7, 8, 9]. To investigate this experimentally, back-to-back  $\Lambda\bar{\Lambda}$  pairs with  $z > 0.15$  are used. The asymmetry between decays with parallel and antiparallel proton and antiproton projections along the normal to the scattering plane is an estimator of the spin correlation. However, after integrating over all angles and applying dilution factors, the expected size of the estimator is smaller than 1%. Since the estimator is measured to be  $-0.10 \pm 0.11$ , the data are found to have too little sensitivity for a measurement of this effect.

## 8 Conclusions

The longitudinal polarization of  $\Lambda$  baryons from Z decay is measured to be  $-0.32 \pm 0.07$  for  $z > 0.3$ . The predicted value based on the standard model and the constituent quark model is  $-0.39 \pm 0.08$ , in good agreement with the measurement.

In addition, the  $\Lambda$  transverse polarization has been studied. The data indicate a signal for  $\Lambda$  transverse polarization above the two  $\sigma$  level.

## Acknowledgement

We wish to thank our colleagues in the CERN accelerator division for operating the LEP machine. We are also grateful to the engineers and technicians in all our institutions for their contribution to the success of ALEPH. Those of us from non-member states thank CERN for its hospitality.

## References

- [1] T. Sjöstrand and M. Bengtsson, *Comp. Phys. Comm.* **39** (1986) 367.
- [2] G. Gustafson and J. Häkkinen, *Phys. Lett.* **B303** (1993) 350.
- [3] D. Adams et al. (SMC Collaboration), *Phys. Lett.* **B329** (1994) 399;  
K. Abe et al. (SLAC-E143 Collaboration), *Phys. Rev. Lett.* **74** (1995) 346.
- [4] L. Montanet et al. (Particle Data Group), *Phys. Rev.* **D50** (1994) 1730.
- [5] A.D. Panagiotou, *Int. J. Mod. Phys.* **A5** (1990) 1197.
- [6] W. Lu, “Novel structure function for photon fragmentation into a  $\Lambda$  hyperon and transverse  $\Lambda$  polarization in unpolarized electron-positron annihilation”, IHEP Beijing, hep-ph/9505361.
- [7] A.V. Efremov, L. Ankwiewics and N.A. Tornquist, *Phys. Lett.* **B284** (1992) 394.
- [8] X. Artru and J. Collins, “Measuring transverse spin correlations by 4-particle correlations in  $e^+ + e^- \rightarrow 2$  jets”, PSU/TH/158, hep-ph/9504220.

- [9] K. Chen, G.R. Goldstein, R.L. Jaffe and X. Ji, Nucl. Phys. **B445** (1995) 380.
- [10] D. Buskulic et al. (ALEPH Collaboration), Nucl. Instr. Meth. **A294** (1990) 121.
- [11] D. Buskulic et al. (ALEPH Collaboration), Nucl. Instr. Meth. **A360** (1995) 481.
- [12] D. Buskulic et al. (ALEPH Collaboration), Z. Phys. **C64** (1994) 361.
- [13] B. Rensch, “Produktion der neutralen seltsamen Teilchen  $K^0$  and  $\Lambda$  in hadronischen  $Z$ -Zerfällen am LEP-Speicherring”, PhD Thesis, Universität Heidelberg, Sept 1992.
- [14] J.E. Campagne and R. Zitoun, Z. Phys. **C43** (1989) 469.
- [15] D. Buskulic et al. (ALEPH Collaboration), Z. Phys. **C55** (1992) 209.
- [16] J.G. Korner, A. Pilaftsis and M.M. Tung, Z. Phys. **C63** (1994) 575.
- [17] G. Marchesini et al., Comp. Phys. Comm. **67** (1992) 465.
- [18] (LEP EW Working Group), “Combined preliminary data on  $Z$  parameters from the LEP experiments and constraints on the standard model”, CERN-PPE/94-197.
- [19] P. Abreu et al. (DELPHI Collaboration), Z. Phys. **C67** (1995) 1.
- [20] D. Buskulic et al. (ALEPH Collaboration), Z. Phys. **C66** (1995) 355.
- [21] P.D. Acton et al. (OPAL Collaboration), Phys. Lett. **B291** (1993) 503.
- [22] P. Abreu et al. (DELPHI Collaboration), Z. Phys. **C67** (1995) 543.
- [23] D. Buskulic et al. (ALEPH Collaboration), “Hyperon production in  $Z$  decays”, EPS0419 contributed paper to the EPS-HEP 95 Conference.
- [24] D. Buskulic et al. (ALEPH Collaboration), “Measurement of the  $\Lambda_b$  polarization in  $Z$  decays”, CERN-PPE/95-156.
- [25] A.F. Falk and M.E. Peskin, Phys. Rev. **D49** (1994) 3320.
- [26] M. Bishai et al. (CLEO Collaboration), Phys. Lett. **B350** (1995) 256.
- [27] D. Crawford et al. (CLEO Collaboration), Phys. Rev. Lett. **75** (1995) 624.

$z$	$P_L^\Lambda$	$p_T$ (GeV/ $c$ )	$P_T^\Lambda$
0.1 – 0.15	$-0.029 \pm 0.024$	0.3 – 0.6	$0.006 \pm 0.014$
0.15 – 0.2	$-0.113 \pm 0.036$	0.6 – 0.9	$0.035 \pm 0.015$
0.2 – 0.3	$-0.085 \pm 0.041$	0.9 – 1.2	$0.000 \pm 0.017$
0.3 – 0.4	$-0.263 \pm 0.072$	1.2 – 1.5	$0.024 \pm 0.019$
0.4 – 1.0	$-0.432 \pm 0.100$	$> 1.5$	$0.015 \pm 0.012$

Table 1: The polarization of  $\Lambda$ 's from Z decay. The longitudinal polarization is binned in  $z = p_\Lambda/p_{\text{beam}}$ , while the transverse polarization is binned in the  $\Lambda$  transverse momentum with respect to the thrust axis. The numbers are averages over  $\Lambda$  and  $\bar{\Lambda}$  such that a positive sign on the longitudinal polarization refers to positive helicity for  $\Lambda$  and negative helicity for  $\bar{\Lambda}$ , while a positive sign on the transverse polarization refers to a positive spin projection along the  $\text{thrust} \times \Lambda(\bar{\Lambda})$  direction. The errors include systematic errors.

$z$	background	$K^0/\Lambda$ resolving	acceptance slope	statistics
0.1 – 0.15	0.004	0.010	0.001	0.021
0.15 – 0.2	0.006	0.010	0.017	0.029
0.2 – 0.3	0.010	0.010	0.023	0.031
0.3 – 0.4	0.012	0.005	0.049	0.051
0.4 – 1.0	0.020	0.005	0.063	0.075

Table 2: Contributions to the experimental uncertainties on the  $\Lambda$  longitudinal polarization.

$z$	$\langle z \rangle$	$A_{\text{FB}}^\Lambda(\text{measured})$	$A_{\text{FB}}^\Lambda(\text{JETSET})$
0.1 – 0.15	0.122	$0.0105 \pm 0.0064$	0.015
0.15 – 0.2	0.173	$0.0300 \pm 0.0080$	0.023
0.2 – 0.3	0.241	$0.0402 \pm 0.0090$	0.039
0.3 – 0.4	0.342	$0.061 \pm 0.016$	0.060
0.4 – 1.0	0.495	$0.130 \pm 0.022$	0.080

Table 3: Forward–backward asymmetry of  $\Lambda$ 's. The errors include systematic errors.

Source of $\Lambda$	$z > 0.3$	$z > 0.15$	Polarization
fragmentation	20%	47%	0
$\Xi \rightarrow \Lambda$	3%	7%	-0.06
$u$	4%	2%	0
$d$	5%	3%	0
$s \rightarrow \Lambda$	31%	13%	-0.91
$s \rightarrow \Xi$	4%	2%	-0.50
$s \rightarrow \Sigma^0$	4%	1%	-0.10
$s \rightarrow \Sigma^*$	16%	7%	-0.50
$c, b$ baryon	7%	8%	-0.25
$c, b$ meson	6%	9%	0

Table 4: Relative contributions to the  $\Lambda$  sample in JETSET, corrected as described in the text, and the predicted longitudinal polarization from each source. The two first rows refer to  $\Lambda$ 's without a primary quark and the following rows to  $\Lambda$ 's containing a primary quark or a primary quark descendant from weak decays.



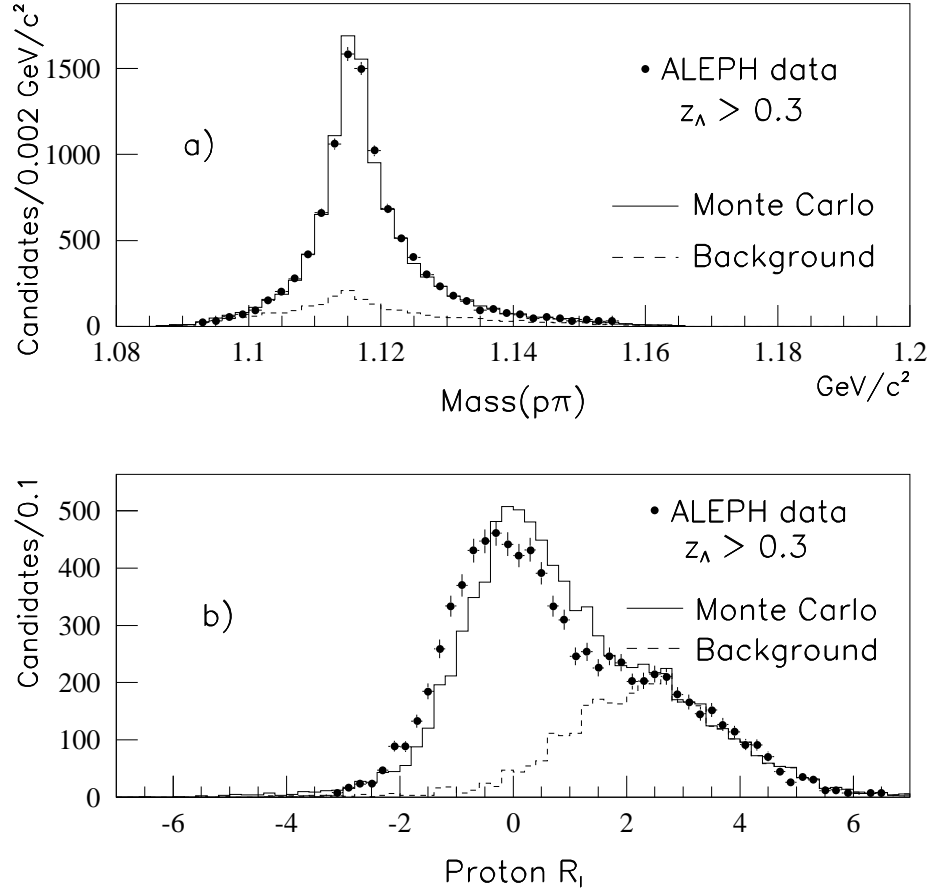


Figure 1: a) The invariant mass distribution of the final  $\Lambda \rightarrow p\pi$  sample at very high momentum. b) The distribution of  $R_I = (I_{\text{meas}} - I_{\text{expect}})/\sigma_I$ , where  $I_{\text{meas}}$  is the measured ionization,  $dE/dx$ , on the proton track,  $I_{\text{expect}}$  is the ionization expected for a proton and  $\sigma_I$  is the resolution of the ionization measurement. The  $\Lambda$  candidates in this figure satisfy all selection criteria except for those involving  $dE/dx$ .

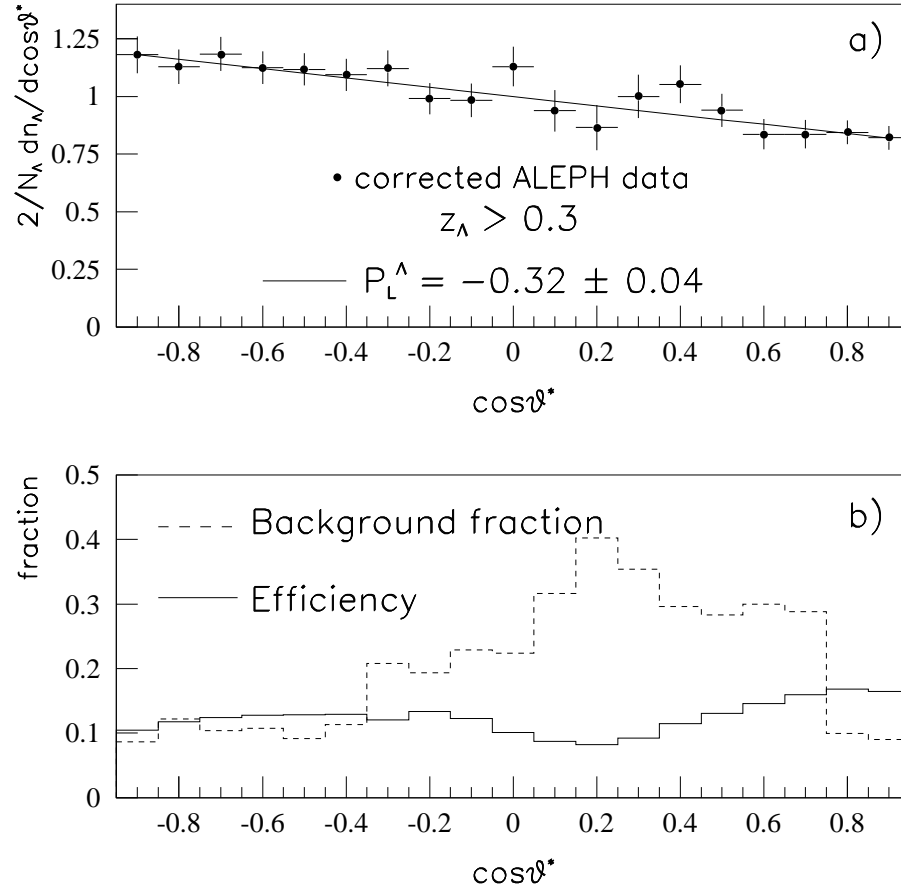


Figure 2: a) Fit of the longitudinal  $\Lambda$  polarization to the corrected decay angle distribution for  $z > 0.3$ . b) Efficiency and background fraction to the  $\Lambda \rightarrow p\pi^-$  sample with  $z > 0.3$ .

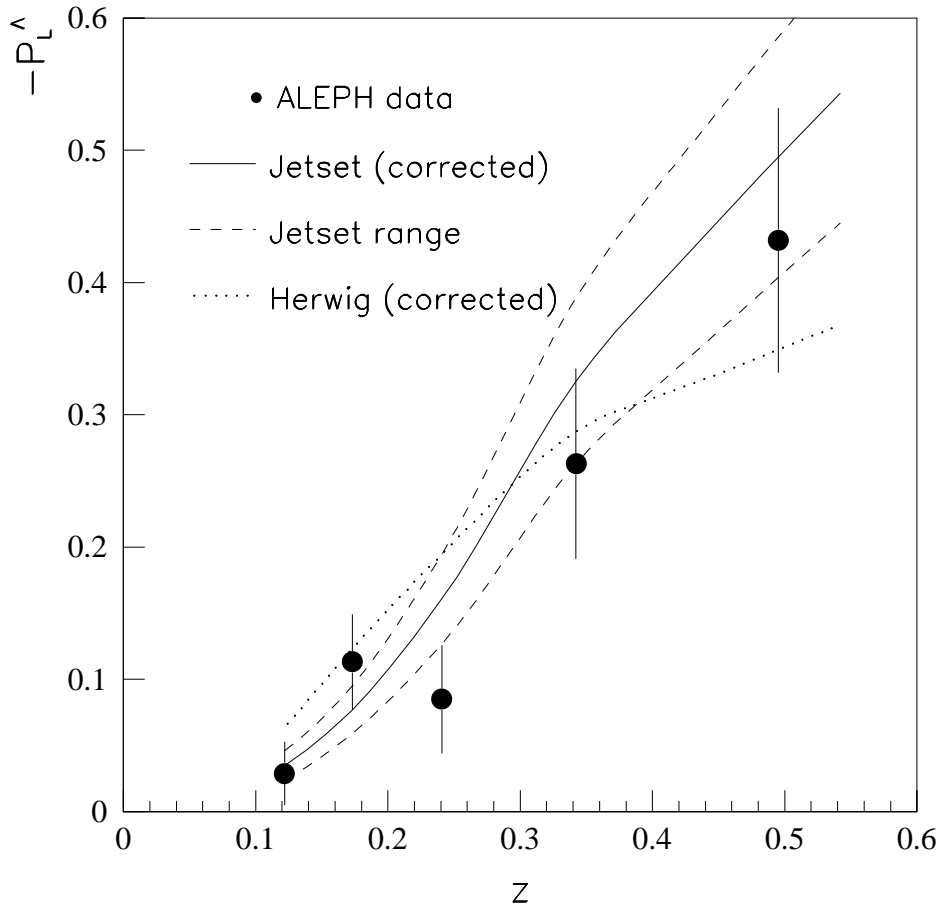


Figure 3: The measured longitudinal  $\Lambda$  polarization is shown as dots. The JETSET prediction after multiplying by a correction factor of 1.07 is shown as a solid line. The dashed lines indicate the estimated uncertainty of the JETSET prediction. The HERWIG prediction after multiplication by a correction factor of 2.17 is shown as a dotted line.

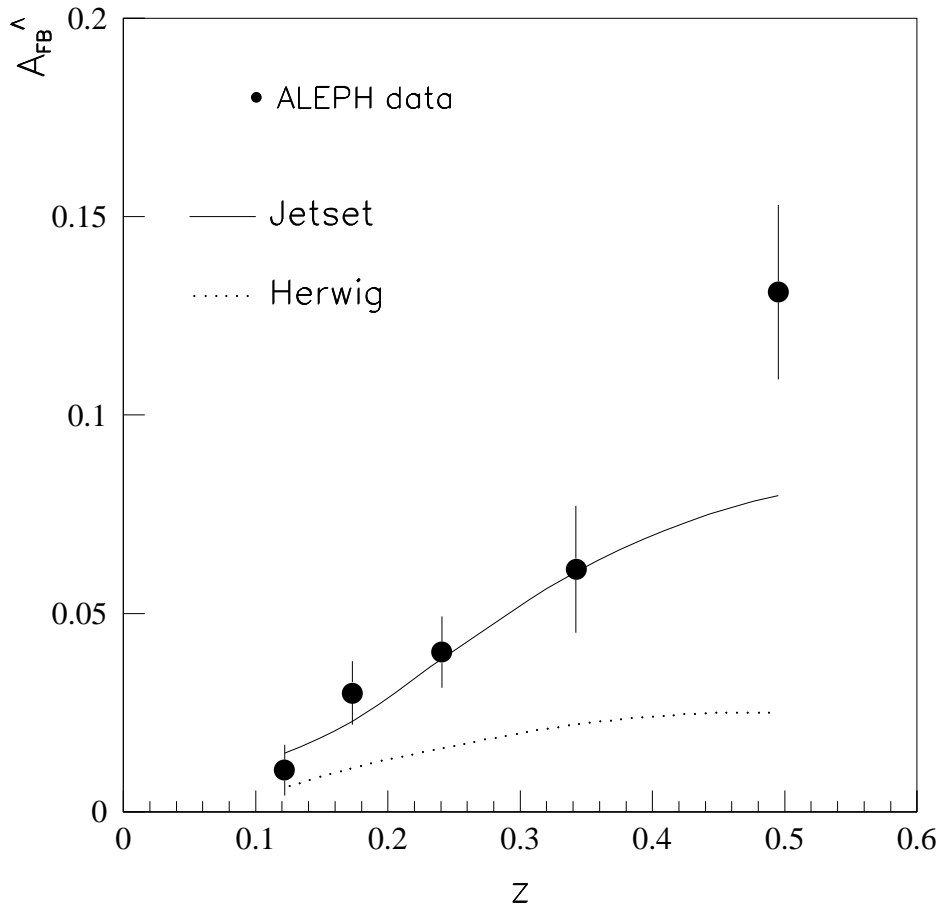


Figure 4: The measured forward-backward asymmetry of  $\Lambda$ 's (dots) together with predictions using JETSET and the standard model fit to LEP measurements (solid curve). The HERWIG prediction is shown as a dotted curve.

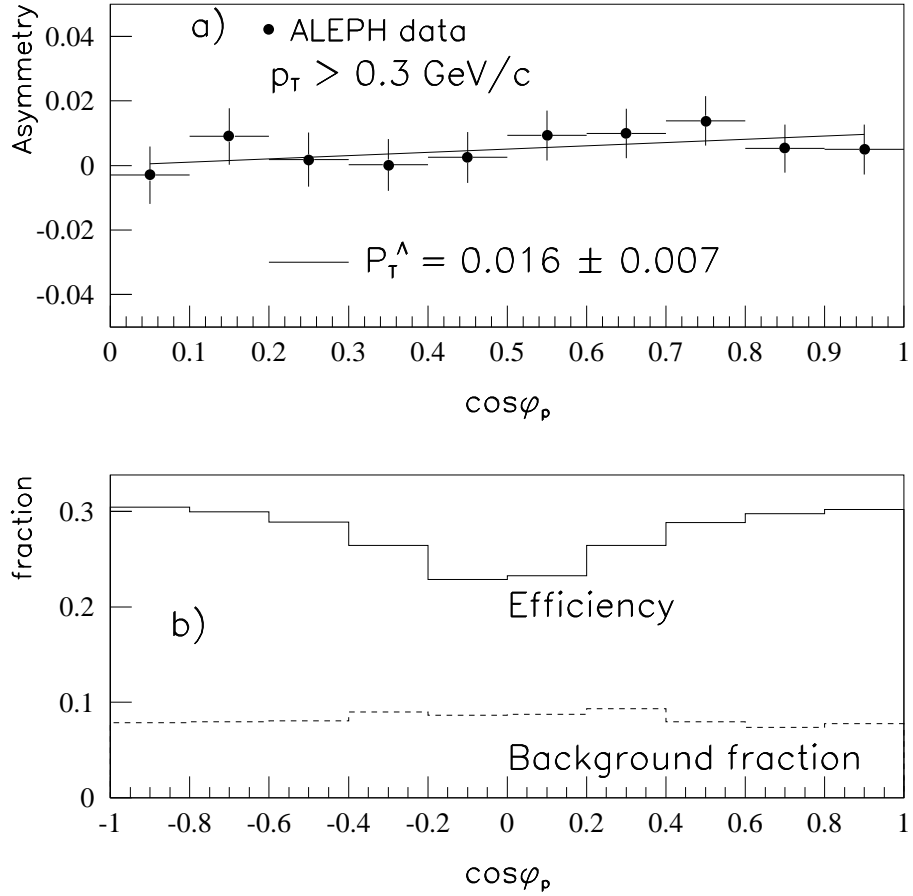


Figure 5: a) Fit of the transverse  $\Lambda$  polarization to data with  $p_T > 0.3 \text{ GeV}/c$ . b) Efficiency and background fraction to the  $\Lambda \rightarrow p\pi^-$  sample with  $p_T > 0.3 \text{ GeV}/c$ .